Small bowel to closest human body surface distance calculation through a custom-made software using CT-based datasets

Marcello Chiurazzi*, *Member, IEEE,* Angelo Damone*, Martina Finocchiaro*, Francesca Farnesi, Giacomo Lo Secco, Edoardo Forcignanò, Alberto Arezzo, Gastone Ciuti, Senior *Member, IEEE*

Abstract—Screening of the gastrointestinal tract is imperative for the detection and treatment of physiological and pathological disorders in humans. Ingestible devices (*e.g.,* magnetic capsule endoscopes) represent an alternative to conventional flexible endoscopy for reducing the invasiveness of the procedure and the related patient's discomforts. However, to properly design localization and navigation strategies for capsule endoscopes, the knowledge of anatomical features is paramount. Therefore, authors developed a semi-automatic software for measuring the distance between the small bowel and the closest human external body surface, using CT colonography images. In this study, volumetric datasets of 30 patients were processed by gastro-intestinal endoscopists with the dedicated custom-made software and results showed an average distance of 79.29 ± 23.85 mm.

Clinical Relevance—The mean distance between the small bowel and the closest human external body surface is calculated, and it equals to 79.29 ± 23.85 mm.

I. INTRODUCTION

Gastrointestinal (GI) diseases represent a widespread problem in developed countries, significantly contributing to the increase of morbidity, mortality and healthcare-related costs [1]–[3]. Ranging from moderate to severe, GI disorders can be acute or chronic, leading patients to periodic examinations. Systematic screening programs are promoted worldwide for the prevention of GI pathologies, especially cancers, indicating the importance of undergoing regular inspection of the stomach and large intestine [4]–[6]. In addition, as demonstrated in the last few years, the alteration of the gut's microbial composition (*i.e.,* microbiota) is associated to several pathologies (*e.g.*, diabetes, obesity, cardio-vascular disorders [7], [8]). Hence, a GI microbial analysis can have a notable impact for a longitudinal and personalized healthcare approach [9].

In this context, the rapid technological advancements in the field of ingestible electronics and capsule endoscopy (CE) represent a powerful tool for the analysis, diagnosis and treatment of GI diseases [10]–[13]. Indeed, CE has the potential to drastically reduce the invasiveness of the procedure, consequential discomfort and the risk of infections and complications. In addition, CE allows to reach portions of the GI tract (*e.g.*, small bowel), not easily accessible through commonly used methodologies (*i.e.,* flexible endoscopy).

Finally, CE provides a methodology to boost personalized medical care, being potentially able to collect multi-modal data [14], towards a P5 medicine approach to oncology [9].

From the first commercially available capsule endoscope on the market in 2001, *i.e.* Pillcam™ from Given Imaging Inc. (Yokne'am Illit, Israel), now part of Medtronic Inc. company (Dublin, Ireland), a wide range of capsule endoscopes have been designed and developed [12], [15]–[17]. Video endoscopy represents only one of the potential applications of these miniaturized systems, which also address: (1) sensing of different parameters (*e.g.,* pressure, temperature, pH, *etc.*) [18], (2) drugs and delivery of treatments [19], and (3) tissue/microbiota sampling [20].

Besides the capsule design, a crucial role in the evolution of this technology is played by the development of robust localization and remote navigation/activation systems, enabling *in-situ* diagnosis and active treatments [21], [22]. Indeed, a major problem in CE is the lack of its ability to target specific sites in the GI tract. Possible solutions include, for instance, the use of magnetic manipulation, enabled by the coupling of external magnetic sources with small magnetic components included into the capsule [23]. However, to design remote navigation controllers or localization systems, it is crucial to know the operational distances, *i.e.* the distance between the capsule, hence the anatomical lumen, and the human external body surface. As a matter of fact, this information, that is so far lacking in the literature, is paramount for the correct dimensioning, design and set-up of such ingestible devices, external controllers and related magnetically-driven navigation/activation strategies. On this regards, this paper aims at covering the aforementioned gap by calculating the distances between the small bowel (our first target) and the human body surface. This is done thanks to an analysis performed by medical doctors (*i.e.,* GI endoscopists) on the abdominal CT colonography datasets from a consecutive series of 30 patients. In this context, a user-friendly and medical-oriented software, developed for the visualization and used for the semi-automatic measurement of the anatomical distances, is here presented.

*These authors equally contributed to the paper.

M. Chiurazzi, A. Damone, M. Finocchiaro and G.Ciuti are with The BioRobotics Institute and the Department of Excellence in Robotics & AI, Scuola Superiore Sant'Anna, 56127 Pisa, Italy (e-mail: marcello.chiurazzi@santannapisa.it, angelo.damone@santannapisa.it, martina.finocchiaro@upc.edu, gastone.ciuti@santannapisa.it).

M. Finocchiaro is also with Center of Research in Biomedical Engineering, Universitat Politecnica de Catalunya, 08034 Barcelona, Spain.

F. Farnesi, G. Lo Secco, E. Forcignanò, A. Arezzo are with Department of Surgical Sciences, University of Torino, 10124 Torino, Italy. (e-mail: ffarnesi1@gmail.com, giacomo.losecco@gmail.com, edoardo.forcignano@edu.unito.it, alberto.arezzo@mac.com).
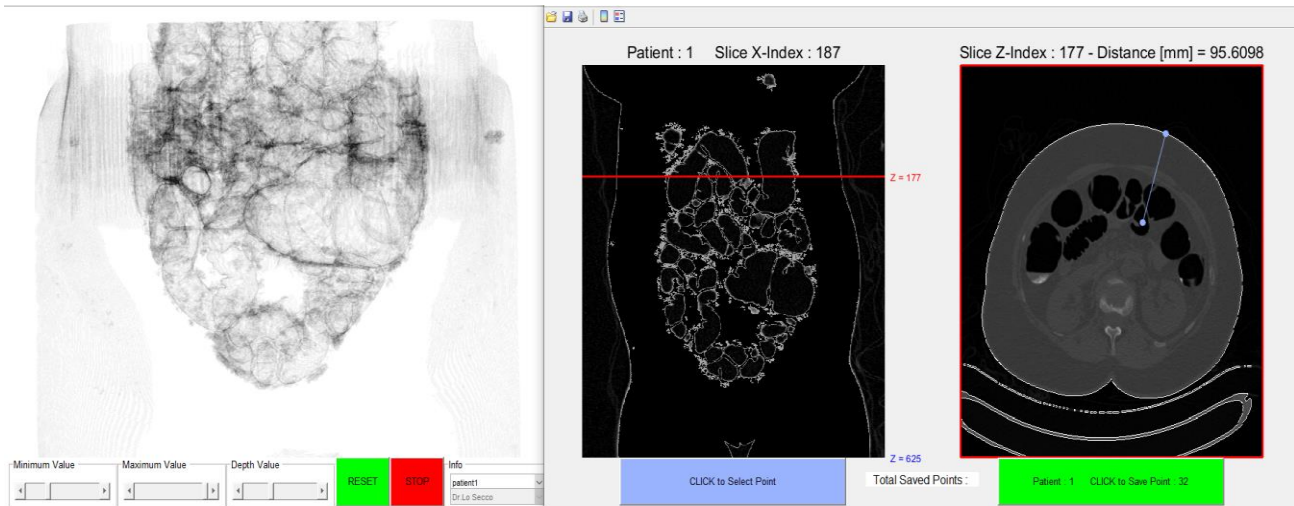
Figure 1 - User-oriented Human Machine Interface for 3D reconstruction, visualization, and semi-automatic distance computation.

II. MATERIALS & METHODS

A. 3D reconstruction of the small bowel from CT images

A custom-made software to easily visualize the GI tract (Figure 1) was designed, starting from images of CT colonography, collected from a public online archive [24]. For each patient's dataset (total: 30 datasets), a 3D model reconstruction of the intestinal lumen (*i.e.,* small bowel and colon) was implemented in Matlab R2020 (MathWorks Inc., Natick, MA, USA). Starting from the available DICOM dataset, belonging to each specific patient, two meaningful images were selected and used to create the mask, later employed to segment the intestine from all the other tissues and internal organs arose from the screening phase. A specific image belonging to the DICOM dataset was used for creating the mask along the transversal plane, whereas a second image was reconstructed starting from the initial dataset (from 512*512*N slices to 512*N slices*512) and used for the mask along the frontal plane. Masks were created using the *Image Segmenter app* of Matlab that allows to create a segmentation mask using either automatic algorithms (*e.g.*, flood fill), semi-automatic techniques (*e.g.*, graph cut), or manual techniques (*e.g.*, drawing ROIs). In addition, it is possible to refine masks using morphology or iterative approaches, such as active contours. In our case, a graph cut procedure has been adopted. Such approach requires selecting the foreground and the background from representative images in order to perform a graph-based segmentation. Despite its limitation in real-time scenarios, this type of segmentation algorithm is able to create, off-line, a resolute mask, that is later used by the Matlab active contour function. This function applies the mask to the entire volume (size*number of images) after being enhanced in contrast using a histogram equalization. Due to the application, a *Chan-Vese* method was applied to define the active contour [25]. Indeed, if object regions are not of significantly different grayscale intensities, the *Chan-Vese* method allows to segment all the objects in the image. For instance, if the image contains some objects that are brighter than the background, and some that are darker, this method typically segments out either the dark or the bright objects only. The workflow of the reconstruction of the volume is reported in Figure 2-left.

B. Graphical User Interface

A software, endowed with an easy-to-use graphical user interface (GUI) was developed, in close collaboration with medical doctors (following a human-centered approach) for interactively selecting representative references of the small bowel. As shown in Figure 1-left, the left part of the GUI displays the reconstructed volumes. This is implemented by using the Matlab *Volume Viewer* function, which allows to plot and simultaneously interact (*e.g.,* rotate, zoom *etc.*) with the 3D reconstruction of the segmented images. In this panel, the user can navigate across different patients, and for each of them, can partition the volume to reconstruct (Figure 1-left). Whereas, on the right side of the GUI, (Figure 1-right), the 2D representation of a specific slice of the reconstructed volume on both the transversal and the frontal planes is shown. This part of the interface enables the user to select the representative points, marking the centers of the small bowel. The algorithm, described in the Section II.C, is then used for computing the minimum distance between the selected points and the human body surface.

C. Semi-automatic computation of distances between the small bowel and the human body surface

The main function of the algorithm for enabling the automatic distance measurement is a *Sobel* operator for edge detection [26]. The Sobel operator uses an isotropic discrete differentiation 3x3 kernel applied, with a convolutional approach, to the pixel intensity of the image, computing an approximated gradient of the intensity. The advantage of this methodology is that it does not require a massive number of computational resources because the kernel operator can be used in both vertical and horizontal directions relative to the pixel grid.

The implemented algorithm measures the distance between a point selected by the user on the small bowel and the closest point belonging to the human body surface, identified as the

TABLE 1 - RESULTS FROM THE DATA ANALYSIS RELATED TO THE DISTANCES MEASURED BETWEEN THE CENTERS OF THE SMALL BOWEL AND THE CLOSEST BODY SURFACE

Dataset	Number of patients	Number of points (sample size)	Mean value (mm)	Standard deviation (mm)	Median (mm)	25th percentile (mm)	75th percentile (mm)	Max value (mm)	Min value (mm)
All data	30	2700	79.29	23.85	80.17	62.01	96.44	153.48	6.67
Occluded	23	2070	76.35	22.67	77.47	60.49	93.00	144.34	6.67
Not occluded	7	630	88.9	25.10	90.15	71.21	105.98	153.48	33.18

skin. Then, the *Sobel* filter is applied to locate the boundary between the human body surface and the external "empty spaces" in the image. Before using the *Sobel* filter to find the edges, the algorithm executes a cleaning background operation by defining a mask to isolate the empty spaces outside the human external body. These empty areas usually are identified as a low pixel intensity on the image, and they are set to a value of zero. Besides, the pixel intensities that identify the human body are set to the maximum value to create a contrast between the "empty space" and the human body to emphasize the application of the *Sobel* filter. For a correct identification of the pixel inside the human body, a morphological image analysis has been used to fill the possible "holes" and make the pixel intensities uniform [27]. Once the external "empty spaces" and the "human body surface" are identified, the algorithm applies the *Sobel* filter to define the edges of the human body and save the edge pixels' position inside a matrix employed to compute the distance from the selected points in the small bowel. The final step of the algorithm is to measure the distance by picking the pixel point representing the manually-selected small bowel's internal part. Once the point is selected by the user, the algorithm finds the closest edge pixel iteratively by computing the norm between the selected point and the pixels that represents the edge, by knowing the grid size in x and y directions. The algorithm operations can be observed in the mask along the frontal plane in the second raw image. The human body surface is highlighted, setting the pixel intensity to the maximum value. A straight line is drawn after the point on the small bowel is selected, and the edge pixel is identified. In Figure 2-right the workflow of the algorithm is presented.

D. Experimental study

Three GI endoscopists were enrolled to perform the tests, using the application described in Section II.B. Each endoscopist was asked to detect 30 points along the center line of the small bowel of each transversal section of the patient's dataset. Overall, 30 consecutive CT datasets were analyzed. For each dataset, the endoscopists were asked to mark the center of the lumen on different transversal 2D slices and to cover, as much as possible, the entire length of the volumetric
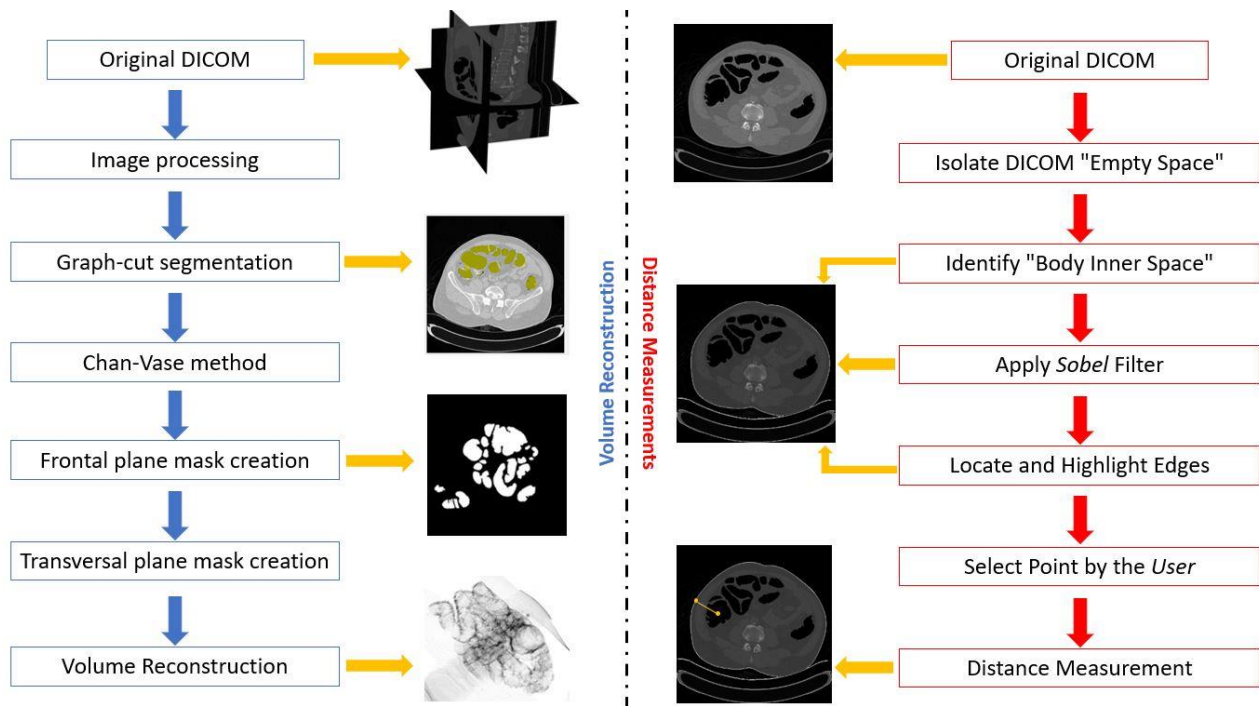

Figure 2 - Workflow of the volumetric reconstruction procedure (left), and distance measurement (right).

small bowel. To identify the correct spots, the medical doctors took advantage of the reconstructed 3D models of the intestine and the filtered CT scan images. At the end of the experimental session, each user was asked to fill a questionnaire to evaluate the performance of the software (*i.e.,* ability of the algorithm to detect the minimum distance between the selected point and external surface) and the overall experience in terms of easiness (1 - poor to 5 - excellent). In addition, (1) the training time required by the endoscopist to master the software and (2) the average procedural time to conclude the task were calculated by and external observer.

E. Data analysis

The data collected during the experiments were analyzed. The mean value and standard deviation of the distance between the manually-selected small bowel centers and the closest human body surface was calculated. Additionally, other statistical parameters to characterize the data distribution were also computed (see TABLE 1). Among all the 30 patients analysed, a subset presented signs of intestinal occlusion. Therefore, the data collected from occluded patients were compared to those from healthy subjects (identified and confirmed by medical doctors) in other to detect any statistical difference among the measures. On this regard, a two samples student t-test was performed between the two groups. Previously, the two data distribution were tested for normality and equality of variances (*i.e.,* F-test). Finally, data collected from the survey were processed in order to extract the cumulative success rate and the mean qualitative score, together with the quantitative training and procedural time to accomplish the experimental task.

III. RESULTS

At the end of the experimental session, each endoscopist marked 900 spots, corresponding to the centers of the small bowel from the abdominal CT colonography scans of 30

Figure 4. Data distribution of the distances computed between the manually-selected small bowel centers and the closets human body surface on occluded patients versus healthy ones. SB: small bowel.

consecutive patients (30 points per patient), for a total of 2700 points. The *mean distance ± standard deviation* between the lumen centers and the closest external body surface corresponds to $79.29 ± 23.85$ mm (see TABLE 1 and Figure 3).

In a second analysis, aimed at comparing the measures performed on the occluded patients (mean distance ± SD = $88.9 ± 25.10$ mm) versus healthy subjects (mean distance ± SD = $76.35 ± 22.67$ mm), statistically-related significant differences were found. The two samples were tested using a two-sample unequal variance student t-test (*i.e.,* Welch's t-test), with a resulting p-value < 0.001. To assess the test, a valid assumption was made regarding the normality of the two distributions (large samples size, $skewness_{occluded}$ = -0.0659, $skewness_{not\ occluded}$ = 0.0307, see Figure 4 and Figure 5) and non-similar variances (F-test, p-value < 0.001).
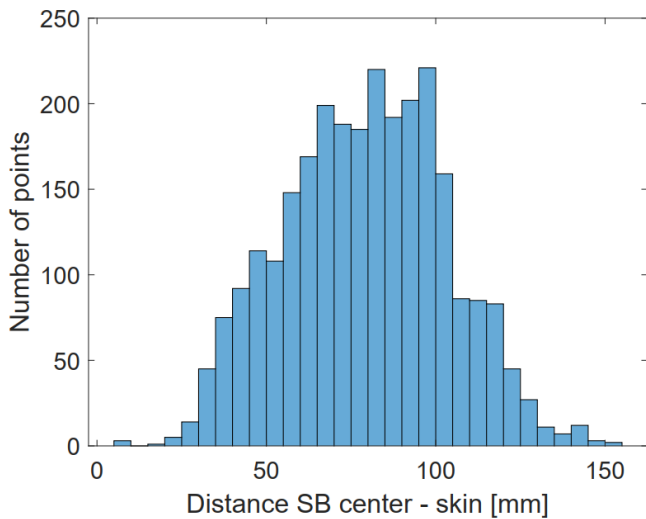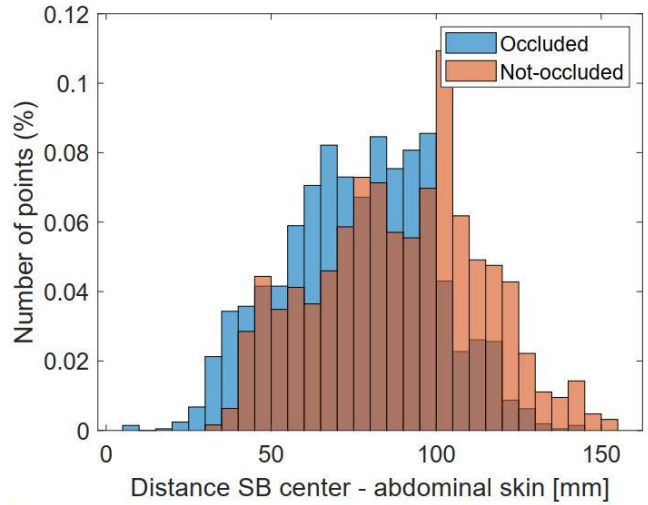

Figure 3. Data distribution of the distances computed between the manually-selected small bowel centers and the closets human body surface. SB: small bowel.
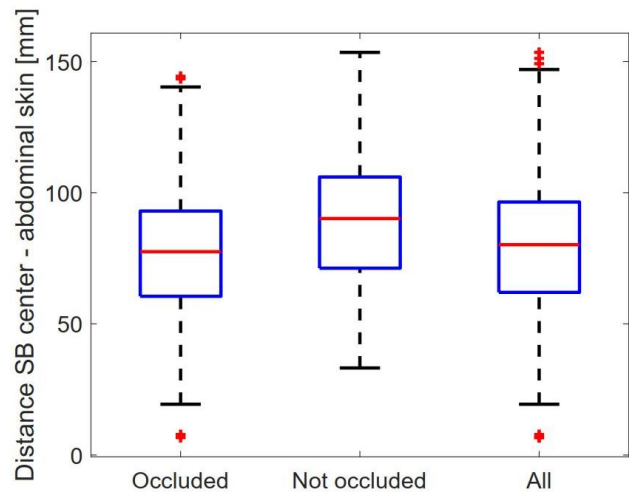

Figure 5 - Comparison of boxplots of the distances computed between the manually-selected small bowel centers and the closets human body surface on occluded, not occluded and all datasets. SB: small bowel.

In addition, as a result of the survey filled by the endoscopists at the end of the study, the easiness of operating the software was rated with the maximum score (5 = "excellent") by all the users. Furthermore, all the endoscopists positively endorsed the ability of the algorithm to correctly detect the minimum distance between the selected point and the human body surface. Finally, the average training time needed by the users to master the software was calculated equal to $0:12 \pm 0:3$ h (mean ± SD), while the average procedural time to conclude the task was calculated as $4:28 \pm 0:17$ h (mean ± SD).

IV. CONCLUSION AND DISCUSSION

The present study enabled the collection of fundamental information related to the anatomy of the human body, that were, to date, absent in the scientific state of the art literature. As a matter of fact, the distance between the center of the small bowel and the human body surface, was never derived before, making an accurate and engineering design of remote controllers for CE and localization strategies hard, if not impossible. This is particularly relevant for CE with magnetic actuation, to enable active navigation [28], [29], wireless activation [30], and localization [31]. Indeed, in this case, the strength of the magnetic link between the external magnetic sources (*e.g.*, an external permanent magnet) and the magnets inside the capsule decreases exponentially with the distance [32]. Therefore, knowing the minimum distance between the capsule inside the bowel (small bowel in this study), and the human body surface is paramount to derive how close the external magnet can get to the internal ones, enabling the proper dimensioning of the whole magnetic-driven system [30]. Similar considerations can be done for the localization strategies of CE (*e.g.*, magnetic localization, radio-wave based localization, etc.). Indeed, in several cases, knowing the distance between the transmitter and the receiver is critical to properly design the localization systems [31]. As expected, the distances measured show high variances, since the small intestine occupies a big portion of the abdominal cavity. Therefore, this study provides a range of measures that, together with the minimum distance, can be used for the aforementioned design purposes.

Additionally, this study highlights a difference on the values measured from healthy people with respect to people suffering from intestinal obstruction. The latter, indeed, presents a lower mean distance between the center of the small bowel and the human body surface. Future work will focus on the acquisition of additional measures from healthy subjects, since in the current study patients with signs of intestinal obstruction prevailed.

Furthermore, this paper demonstrates the efficacy of a novel interactive GI tract visualizer also for screening purposes. Such application is the result of an interdisciplinary collaboration between engineers and endoscopists. The software features may place the proposed system as a candidate for enabling both screening and clinically-relevant interactive procedures. As a matter of facts, the simultaneous presence of a 3D reconstruction of the bowel and the 2D representation of specific slices of the volume makes the identification of the anatomical landmarks easier and the analysis of radiologic images faster.

However, the work was mainly focused on the small bowel. Therefore, further efforts should focus on improving the software for a more general purpose. The presented study, indeed, may pave the way to an extended analysis of the mean distances of the entire intestine (also including the colon) from the human body surface. Starting from such information, researchers will be able to reliably design and set-up magnetic remote controllers and localization systems, to track online ingestible capsules, and eventually allowing *in-situ* activation and delivery of specific treatments.

BIBLIOGRAPHY

[1]   G. Holtmann, A. Shah, and M. Morrison, "Pathophysiology of Functional Gastrointestinal Disorders: A Holistic Overview," *Digestive Diseases*, vol. 35, no. 1. S. Karger AG, pp. 5–13, Mar. 01, 2018, doi: 10.1159/000485409.

[2]   A. Săftoiu *et al.*, "Role of gastrointestinal endoscopy in the screening of digestive tract cancers in Europe: European Society of Gastrointestinal Endoscopy (ESGE) Position Statement," *Endoscopy*, vol. 52, no. 4, pp. 293–304, Apr. 2020, doi: 10.1055/a-1104-5245.

[3]   D. Ang, K. M. Fock, N. M. Law, and T. L. Ang, "Current status of functional gastrointestinal evaluation in clinical practice," *Singapore Med. J.*, vol. 56, no. 2, pp. 69–80, 2015, doi: 10.11622/smedj.2015021.

[4]   "The top 10 causes of death." https://www.who.int/news-room/fact-sheets/detail/the-top-10-causes-of-death (accessed Jan. 24, 2021).

[5]   A. N. Ananthakrishnan and R. J. Xavier, "Gastrointestinal Diseases," in *Hunter's Tropical Medicine and Emerging Infectious Diseases*, Elsevier, 2020, pp. 16–26.

[6]   L. Johnson, F. Ghishan, J. Kaunitz, J. Merchant, H. Said, and J. Wood, *Physiology of the Gastrointestinal Tract*, vol. 1–2. Elsevier Inc., 2012.

[7]   E. N. Janoff, "The microbiome and human disease pathogenesis: how do you do what you do to me …?," *Translational Research*, vol. 179. Mosby Inc., pp. 1–6, Jan. 2017, doi: 10.1016/j.trsl.2016.10.007.

[8]   E. Thursby and N. Juge, "Introduction to the human

gut microbiota," *Biochemical Journal*, vol. 474, no. 11. Portland Press Ltd, pp. 1823–1836, Jun. 2017, doi: 10.1042/BCJ20160510.

[9]   G. Cummins *et al.*, "Gastrointestinal diagnosis using non-white light imaging capsule endoscopy," *Nature Reviews Gastroenterology and Hepatology*, vol. 16, no. 7. Nature Publishing Group, pp. 429–447, Jul. 01, 2019, doi: 10.1038/s41575-019-0140-z.

[10]   C. Steiger, A. Abramson, P. Nadeau, A. P. Chandrakasan, R. Langer, and G. Traverso, "Ingestible electronics for diagnostics and therapy," *Nature Reviews Materials*, vol. 4, no. 2. Nature Publishing Group, pp. 83–98, Feb. 01, 2019, doi: 10.1038/s41578-018-0070-3.

[11]   W. Marlicz *et al.*, "Frontiers of Robotic Gastroscopy: A Comprehensive Review of Robotic Gastroscopes and Technologies," *Cancers (Basel).*, vol. 12, no. 10, p. 2775, Sep. 2020, doi: 10.3390/cancers12102775.

[12]   G. Ciuti *et al.*, "Frontiers of Robotic Colonoscopy: A Comprehensive Review of Robotic Colonoscopes and Technologies," *J. Clin. Med.*, vol. 9, no. 6, p. 1648, May 2020, doi: 10.3390/jcm9061648.

[13]   A. Gorini and G. Pravettoni, "P5 medicine: A plus for a personalized approach to oncology," *Nature Reviews Clinical Oncology*, vol. 8, no. 7. Nature Publishing Group, p. 444, Jul. 31, 2011, doi: 10.1038/nrclinonc.2010.227-c1.

[14]   S. S. Mapara and V. B. Patravale, "Medical capsule robots: A renaissance for diagnostics, drug delivery and surgical treatment," *Journal of Controlled Release*, vol. 261. Elsevier B.V., pp. 337–351, Sep. 10, 2017, doi: 10.1016/j.jconrel.2017.07.005.

[15]   K. Kalantar-Zadeh, N. Ha, J. Z. Ou, and K. J. Berean, "Ingestible Sensors," *ACS Sensors*, vol. 2, no. 4. American Chemical Society, pp. 468–483, Apr. 28, 2017, doi: 10.1021/acssensors.7b00045.

[16]   F. Munoz, G. Alici, and W. Li, "A review of drug delivery systems for capsule endoscopy," *Advanced Drug Delivery Reviews*, vol. 71. Elsevier, pp. 77–85, 2014, doi: 10.1016/j.addr.2013.12.007.

[17]   Q. Tang *et al.*, "Current Sampling Methods for Gut Microbiota: A Call for More Precise Devices," *Frontiers in Cellular and Infection Microbiology*, vol. 10. Frontiers Media S.A., p. 151, Apr. 09, 2020, doi: 10.3389/fcimb.2020.00151.

[18]   D. O. Otuya *et al.*, "Non-endoscopic biopsy techniques: a review," *Expert Rev. Gastroenterol. Hepatol.*, vol. 12, no. 2, pp. 109–117, Feb. 2018,

doi: 10.1080/17474124.2018.1412828.

[19]   F. Bianchi *et al.*, "Expert Review of Medical Devices Localization strategies for robotic endoscopic capsules: a review Localization strategies for robotic endoscopic capsules: a review," 2019, doi: 10.1080/17434440.2019.1608182.

[20]   L. Sliker, G. Ciuti, M. Rentschler, and A. Menciassi, "Magnetically driven medical devices: A review," *Expert Review of Medical Devices*, vol. 12, no. 6. Taylor and Francis Ltd, pp. 737–752, Nov. 02, 2015, doi: 10.1586/17434440.2015.1080120.

[21]   J. Li *et al.*, "Magnetically-driven medical robots: An analytical magnetic model for endoscopic capsules design," *J. Magn. Magn. Mater.*, vol. 452, pp. 278–287, Apr. 2018, doi: 10.1016/J.JMMM.2017.12.085.

[22]   "CT COLONOGRAPHY - The Cancer Imaging Archive (TCIA) Public Access - Cancer Imaging Archive Wiki." https://wiki.cancerimagingarchive.net/display/Public/CT+COLONOGRAPHY (accessed Feb. 22, 2021).

[23]   T. F. Chan and L. A. Vese, "Active contours without edges," *IEEE Trans. Image Process.*, vol. 10, no. 2, pp. 266–277, 2001, doi: 10.1109/83.902291.

[24]   A. Kaur, "A Review Paper on Image Segmentation and its Various Techniques in Image Processing," *Int. J. Sci. Res. ISSN (Online Impact Factor*, vol. 3, no. 12, pp. 2319–7064, 2012.

[25]   P. Soille, *Morphological Image Analysis*. Springer Berlin Heidelberg, 2004.

[26]   M. Verra *et al.*, "Robotic-Assisted Colonoscopy Platform with a Magnetically-Actuated Soft-Tethered Capsule," *Cancers (Basel).*, vol. 12, no. 9, p. 2485, Sep. 2020, doi: 10.3390/cancers12092485.

[27]   J. W. Martin *et al.*, "Enabling the future of colonoscopy with intelligent and autonomous magnetic manipulation," *Nat. Mach. Intell.*, vol. 2, no. 10, pp. 595–606, Oct. 2020, doi: 10.1038/s42256-020-00231-9.

[28]   M. Simi, G. Gerboni, A. Menciassi, and P. Valdastri, "Magnetic torsion spring mechanism for a wireless biopsy capsule," *J. Med. Devices, Trans. ASME*, vol. 7, no. 4, Sep. 2013, doi: 10.1115/1.4025185.

[29]   J. Li *et al.*, "Magnetically-driven medical robots: An analytical magnetic model for endoscopic capsules design," *J. Magn. Magn. Mater.*, vol. 452, pp. 278–287, Apr. 2018, doi: 10.1016/j.jmmm.2017.12.085.